

# Majorana entropy revival via tunneling phases

Sergey Smirnov

*P. N. Lebedev Physical Institute of the Russian Academy of Sciences, 119991 Moscow, Russia\**

(Dated: March 1, 2021)

Measuring the Majorana entropy  $S_M = k_B \log(2^{\frac{1}{2}})$  may uniquely reveal whether an initial equilibrium state of a nanoscale device is of Majorana nature and subsequent operations deal with an essentially nonlocal pair of non-Abelian Majorana bound states and not with trivial or other accidental non-Abelian states. However, in realistic setups both Majorana modes are inevitably involved in tunneling processes. We show that even when the tunneling amplitude of one Majorana mode is significantly suppressed, the Majorana entropy ruins and straightforward experiments will in general detect entropy  $S \ll S_M$ . To avoid this general problem we present a mechanism of the Majorana entropy revival via the tunneling phases of the Majorana modes and demonstrate that to successfully observe the universal Majorana plateau  $S = S_M$  one should intelligently tune the tunneling phases instead of leaving them uncontrolled. Practical feasibility of appropriate Majorana entropy measurements is supported by an example with parameters well achievable in modern labs.

## I. INTRODUCTION

Quantum thermodynamic properties of a nanoscopic system offer a rich source of information about its physical states. For instance, the system's entropy at low temperatures provides the physical nature of the quantum ground states which also determine quantum transport characteristics such as the linear conductance. Thus getting access to thermodynamics of a nanoscopic system is an extremely challenging task for modern experiments to reveal both the system's quantum ground states and how they govern quantum transport response of the system.

This is particularly important for nanoscopic systems involving one-dimensional topological superconductors in their topologically nontrivial phases replicating [1–5] the prototypical phase of the Kitaev model [6] realized, *e.g.*, on the basis of semiconductors with strong spin-orbit interactions [7, 8]. This phase is characterized by non-Abelian Majorana bound states (MBSs) localized at the ends of a topological superconductor appearing after a topological quantum phase transition as a consequence of a qualitative change of the quantum ground state from a trivial one to a nontrivial Majorana state.

The Majorana quantum ground state dictates specific features of quantum transport response such as the linear conductance observed in experiments [9, 10], in particular, its universality [11]. In fact, quantum transport predicts many specific Majorana induced signatures in various characteristics such as thermoelectric currents [12–16], shot noise [17–22], quantum noise [23], thermoelectric shot noise [24], thermoelectric quantum noise [25], tunnel magnetoresistances in ferromagnetic systems [26], linear conductances in quantum dissipative systems [27], quantum transmission in photon-assisted transport [28], pumped heat and charge statistics [29]. Transport prop-

erties may also be combined with thermodynamic ones [30] to observe dual Majorana universality.

Revealing many consequences of the Majorana quantum ground states, quantum transport is, however, unable to directly access the Majorana ground states themselves. To uniquely detect MBSs within quantum transport experiments one should be able to adapt them to mimic Majorana braiding protocols, *e.g.*, by means of nonequilibrium noise measurements [31].

Nevertheless, it is highly appealing to uniquely reveal MBSs directly from the system's quantum ground state avoiding braiding protocols or their conceivable counterparts. Successful experimental entropy measurements [32, 33] provide an exceptional opportunity to access the Majorana entropy in nanoscopic systems. In practice, however, this is not a straightforward task. Indeed, to measure the Majorana entropy one could consider an ideal setup presumably involving a pair of highly non-local non-Abelian MBSs with a finite coupling to only one Majorana mode ignoring completely any coupling to the second Majorana mode as proposed in Refs. [34, 35].

Here we demonstrate that the above idealization will likely fail to guide experimental observations of the Majorana entropy  $S_M = k_B \log(2^{\frac{1}{2}})$  because of inevitable finite coupling to the second Majorana mode in a realistic setup. As discussed below, even if the tunneling amplitude of the second Majorana mode is several orders of magnitude smaller than the tunneling amplitude of the first Majorana mode, straightforward experiments will be essentially brought in a regime with entropy  $S \ll S_M$ . We reveal that such a strong sensitivity of the system's entropy to the coupling of the second Majorana mode is the result of emergence of additional degrees of freedom, namely the Majorana tunneling phases. Exactly these new degrees of freedom, if left uncontrolled, ruin the Majorana entropy to a much smaller value. Remarkably, it turns out that exactly the Majorana tunneling phases provide a revival of the Majorana entropy that is a return of the system to the Majorana quantum ground state with the entropy  $S = S_M$ . As we show, one may revive Majorana quantum ground states via tunneling

\* 1) sergej.physik@gmail.com

2) sergey.smirnov@physik.uni-regensburg.de

3) ssmirnov@sci.lebedev.ru

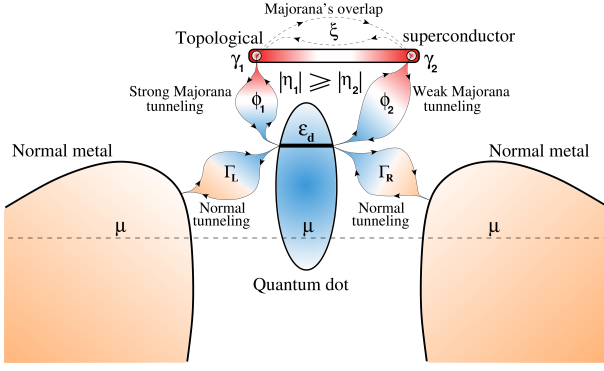


FIG. 1. A nanoscopic system whose quantum thermodynamic and transport properties stem from the nonlocal nature of non-Abelian MBSs.

phases or a gate voltage in setups with experimentally realizable parameters.

The paper is organized as follows. In Section II we present a realistic nanoscopic setup where both Majorana modes are involved in tunneling processes with corresponding tunneling phases which become new parameters of the system's entropy. The dependence of the system's entropy on the tunneling phases is numerically explored in Section III which shows how the Majorana ground state revives via tuning the tunneling phases restoring simultaneously the Majorana values of the entropy and linear conductance. Additionally, we demonstrate how to revive the Majorana state via a gate voltage at fixed arbitrary values of Majorana tunneling phases. We conclude with Section IV where we estimate a possibility of an experimental implementation of the Majorana ground state revival, mention connection to driven dissipative protocols using tunneling phases to control Majorana qubits and also provide an outlook on various systems where Majorana tunneling phases might play an essential role.

## II. THEORETICAL MODEL AND MAJORANA ENTROPY

To specify our discussion let us consider a concrete setup shown in Fig. 1. The system is composed of a quantum dot, two normal massive metals and a grounded topological superconductor with MBSs localized at its ends. The quantum dot interacts with the normal metals and topological superconductor through tunneling mechanisms.

The quantum dot Hamiltonian is

$$\hat{H}_d = \epsilon_d d^\dagger d. \quad (1)$$

The location of the energy level  $\epsilon_d$  with respect to the chemical potential  $\mu$  is tuned by a gate voltage. Both the energy level  $\epsilon_d$  and the chemical potential  $\mu$  are measured with respect to the middle of the induced superconducting gap at which the Majoranas are bound. Below

we focus on the case when the chemical potential coincides with the middle of the induced superconducting gap. Therefore varying  $\epsilon_d$  by a gate voltage with respect to the middle of the induced superconducting gap is identical to varying it with respect to the chemical potential  $\mu$  which has a unique value in equilibrium where it only makes sense to explore the system's entropy. Thus, in what follows, values of  $\epsilon_d$  will be assumed to be given with reference to the chemical potential  $\mu$ . While the impact of deviations of the chemical potential from the middle of the induced superconducting gap will be explored in future research, the case we explore here is also adopted in many other works. For example, in the limit of only one Majorana mode coupled to the quantum dot our Green's functions given below are similar to those in Refs. [17, 18] for the noninteracting setups. In particular, in this limit our Green's functions result in the same values of the linear conductance and shot noise (see Refs. [21, 34]) as those obtained in Refs. [17, 18].

The Hamiltonian of the normal metals,

$$\hat{H}_c = \sum_{l=L,R} \sum_k \epsilon_k c_{lk}^\dagger c_{lk}, \quad (2)$$

is a sum over the left ( $L$ ) and right ( $R$ ) contacts as well as over the momentum index  $k$ . It is characterized by continuous spectra  $\epsilon_k$  resulting in a density of states  $\nu(\epsilon)$  assumed energy independent in the vicinity of the chemical potential,  $\nu(\epsilon) \approx \nu_c/2$ . The normal metals are assumed to be in equilibrium specified by the Fermi-Dirac distribution with the chemical potentials  $\mu_{L,R}$  and temperature  $T$ ,  $f_{L,R}(\epsilon) = \{\exp[(\epsilon - \mu_{L,R})/k_B T] + 1\}^{-1}$ . Below the system's entropy is calculated in equilibrium,  $\mu_L = \mu_R = \mu$ , whereas we calculate the linear conductance for  $\mu_{L,R} = \mu \pm eV/2$ , where  $V$  is an infinitesimal bias voltage between the two normal metals,  $V \rightarrow 0$ .

Here it is appropriate to mention that while the electric current induced by the bias voltage  $V$  is a nonequilibrium characteristic, the linear conductance is a transport property fully specified by the system's equilibrium state. Therefore at low temperatures the behavior of the linear conductance is governed by the system's quantum ground state whose nature is revealed by the system's entropy. Below we will demonstrate that the linear conductance takes the Majorana fractional value when the entropy signals that the system's quantum ground state has acquired the Majorana nature.

The tunneling interaction of the quantum dot with the left and right normal metals is described by the Hamiltonian

$$\hat{H}_{d-c} = \sum_{l=L,R} \mathcal{T}_l \sum_k c_{lk}^\dagger d + \text{H.c.} \quad (3)$$

bringing the energy scale  $\Gamma \equiv \Gamma_L + \Gamma_R$ ,  $\Gamma_l \equiv \pi \nu_C |\mathcal{T}_l|^2$ . Here we have assumed that the tunneling matrix elements do not depend on the momentum index  $k$ . Physically this simplification corresponds to a scabrous tunneling barrier where the tunneling is most intensive at only

one point of the barrier, namely at its thinnest point. Under such physical conditions our simplification is well justified. In the opposite situation of a smooth tunneling barrier having approximately constant width our simplification will not affect the results at low temperatures when the range of relevant energies is very small. Our simplification would probably become less precise for a smooth tunneling barrier at high temperatures when the MBSs are no longer effective. However, at low temperatures, when the Majorana low energy sector governs the system's physical behavior, our results will not be much influenced by that simplification even for a smooth tunneling barrier. We also note that in equilibrium, when  $\mu_L = \mu_R = \mu$ , the two normal metals are indistinguishable and are physically equivalent to a single normal metal. As a result, the system's entropy must not depend on specific values of the energies  $\Gamma_L$  and  $\Gamma_R$  but it must depend only on their sum that is on  $\Gamma$ . In contrast, the value of the linear conductance may depend on specific values of  $\Gamma_L$  and  $\Gamma_R$ . Below, when we calculate the linear conductance, we assume  $\Gamma_L = \Gamma_R = \Gamma/2$ .

The highly nonlocal Majorana modes localized at the ends of the topological superconductor,  $\gamma_1$  and  $\gamma_2$ , are both linked with the quantum dot and may also have a finite overlap between each other. The links of  $\gamma_1$  and  $\gamma_2$  with the quantum dot have, respectively, tunneling amplitudes  $|\eta_1|$  and  $|\eta_2|$  as well as tunneling phases  $\phi_1$  and  $\phi_2$ . The corresponding Hamiltonian is

$$\hat{H}_{d-ts} = \eta_1^* d^\dagger \gamma_1 + \eta_2^* d^\dagger \gamma_2 + \text{H.c.}, \quad (4)$$

where  $\gamma_i^\dagger = \gamma_i$ ,  $\{\gamma_i, \gamma_j\} = 2\delta_{ij}$ ,  $\eta_{1,2} = |\eta_{1,2}| \exp(i\phi_{1,2})$ . The Majorana mode  $\gamma_1$  is linked to the quantum dot stronger than the Majorana mode  $\gamma_2$ , *i.e.*  $|\eta_1| > |\eta_2|$ . The Majorana's overlap, shown by the dashed arrows, is modeled by the Hamiltonian

$$\hat{H}_{ts} = i\xi\gamma_2\gamma_1/2 \quad (5)$$

with the overlap energy scale  $\xi$ . We note that physical observables, in particular the system's entropy, cannot depend separately on the two phases  $\phi_1$  and  $\phi_2$  but they must depend only on their difference  $\Delta\phi \equiv \phi_1 - \phi_2$ .

As in Ref. [34], replacing the second quantized operators in the above Hamiltonians with the corresponding Grassmann fields on the imaginary time axis, the thermodynamic partition function  $Z$  of the system is represented by a field integral in imaginary time with the Grassmann fields subject to the antiperiodic boundary conditions [36]. The system's entropy is then obtained from the thermodynamic potential  $\Omega = -k_B T \log Z$  as the first derivative over the temperature,  $S = -\partial\Omega/\partial T$ . It has the form:

$$S = k_B \log \left[ \cosh \left( \frac{\xi}{2k_B T} \right) \right] - \frac{\xi}{2T} \tanh \left( \frac{\xi}{2k_B T} \right) + k_B \log(2) + \frac{1}{8\pi k_B T^2} \int_{-\infty}^{\infty} d\epsilon \frac{\epsilon \phi(\epsilon)}{\cosh^2(\frac{\epsilon}{2k_B T})}, \quad (6)$$

where  $\phi(\epsilon)$  represents the phase of a complex expression involving the retarded and advanced hole-particle, hole-hole and particle-particle Green's functions,

$$G_{hp}^A(-\epsilon)G_{hp}^R(\epsilon) - G_{hh}^A(-\epsilon)G_{pp}^R(\epsilon) = \rho(\epsilon) \exp[i\phi(\epsilon)], \quad (7)$$

where  $iG_{jj'}^{R,A}(t|t') \equiv \pm\Theta(\pm t \mp t') \langle \{d_j(t), d_{j'}(t')\} \rangle$ ,  $j = p, h$  and  $d_p \equiv d^\dagger$ ,  $d_h \equiv d$ . The last term in Eq. (6) takes into account the tunneling interactions of the quantum dot with the normal metals and topological superconductor while the first three terms may be interpreted as the entropy of a two-level system in which the distance between the two energy levels is equal to  $\xi$ .

The Green's functions depend on the parameters of the above setup, in particular on the tunneling phase difference  $\Delta\phi$ , and are found from a field integral in real time, the Keldysh field integral [36]. The retarded Green's functions have the following form:

$$G_{ij}^R(\epsilon) = \frac{g_{ij}^R(\epsilon)}{g^R(\epsilon)}, \quad (8)$$

where

$$\begin{aligned} g_{hp}^R(\epsilon) &= 2\hbar(\epsilon^2 - \xi^2)[i\Gamma + 2(\epsilon_d + \epsilon)] \\ &\quad - 8\hbar[2\xi|\eta_1||\eta_2|\sin(\Delta\phi) + \epsilon(|\eta_1|^2 + |\eta_2|^2)], \\ g_{pp}^R(\epsilon) &= -8\hbar\epsilon(\eta_1^2 + \eta_2^2), \\ g_{hh}^R(\epsilon) &= -8\hbar\epsilon[(\eta_1^*)^2 + (\eta_2^*)^2], \\ g^R(\epsilon) &= (\xi^2 - \epsilon^2)[4\epsilon_d^2 + (\Gamma - 2i\epsilon)^2] \\ &\quad + 64|\eta_1|^2|\eta_2|^2\sin^2(\Delta\phi) + 32\epsilon_d\xi|\eta_1||\eta_2|\sin(\Delta\phi) \\ &\quad - 8i\epsilon(\Gamma - 2i\epsilon)(|\eta_1|^2 + |\eta_2|^2). \end{aligned} \quad (9)$$

The advanced Green's functions are obtained from the relations:

$$\begin{aligned} G_{hp}^A(\epsilon) &= [G_{hp}^R(\epsilon)]^*, \\ G_{pp}^A(\epsilon) &= [G_{pp}^R(\epsilon)]^*, \\ G_{hh}^A(\epsilon) &= [G_{hh}^R(\epsilon)]^*, \end{aligned} \quad (10)$$

which follow from the definitions of the retarded and advanced hole-particle, hole-hole and particle-particle Green's functions given above.

### III. RESULTS

In Fig. 2 we show the results obtained for the system's entropy as a function of the tunneling phase difference  $\Delta\phi$  in polar coordinates. Specifically, the distance from the center (the origin of coordinates) to a point on a curve is equal to  $S$  while the polar angle is equal to  $\Delta\phi$ . Different curves correspond to different values of a gate voltage controlling  $\epsilon_d$ . The solid red, blue, green, orange and magenta curves show  $S$  for positive values of  $\epsilon_d$  while the dashed blue, green and magenta curves show  $S$  for the corresponding negative values of  $\epsilon_d$ . The solid black

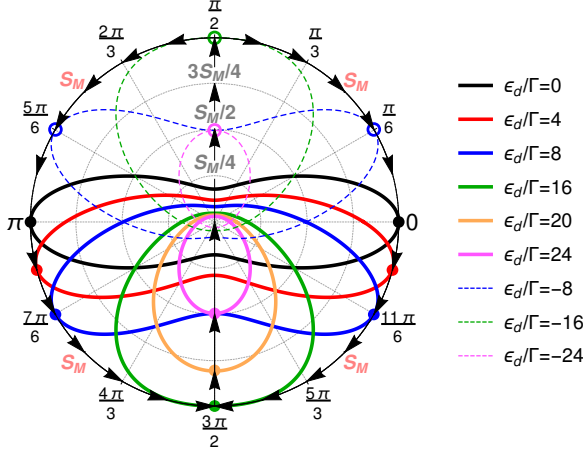


FIG. 2. A plot representing the system's entropy  $S$  as a function of the difference of the tunneling phases,  $\Delta\phi = \phi_1 - \phi_2$ , in polar coordinates. Here the splitting energy in Eq. (11) is  $\epsilon_M/\Gamma = 16$  and thus a single entropy maximum splits into two maxima at  $\epsilon_d = \pm\epsilon_M$ , that is at  $\epsilon_d/\Gamma = \pm 16$  (solid and dashed green curves, respectively).

curve is for  $\epsilon_d = 0$ . Here  $k_B T/\Gamma = 10^{-8}$ ,  $|\eta_1|/\Gamma = 4 \cdot 10^2$ ,  $|\eta_2|/\Gamma = 10^{-4}$ ,  $\xi/\Gamma = 10^{-2}$ . As can be seen, although  $|\eta_1|$  is more than six orders of magnitude larger than  $|\eta_2|$ , all the curves are highly anisotropic showing a very strong dependence of the system's entropy  $S$  on the tunneling phase difference  $\Delta\phi$ . The points on the curves with  $\epsilon_d \geq 0$  and the circles on the curves with  $\epsilon_d < 0$  indicate where  $S$  reaches its maximal value. The radius of the largest polar circle is equal to the Majorana entropy  $S_M$ .

We find numerically that all the curves with  $|\epsilon_d| < \epsilon_M$  touch the largest polar circle  $S_M$  at two points while the curves with  $|\epsilon_d| = \epsilon_M$  touch it only at one point, at  $\Delta\phi = \pi/2$  for  $\epsilon_d < 0$  and at  $\Delta\phi = 3\pi/2$  for  $\epsilon_d > 0$ .

Here there appears a new energy scale,

$$\epsilon_M \equiv \frac{4|\eta_1||\eta_2|}{\xi}, \quad (11)$$

which has been identified numerically for setups with  $|\eta_2| \ll |\eta_1|$ . It is interesting to note that this energy scale and the above mentioned entropy maximum points do not appear in our numerical calculations for setups with  $|\eta_2| \sim |\eta_1|$  which are not explored here but will be a topic of our future research.

For  $|\epsilon_d| > \epsilon_M$  the maximal values of  $S$  start to depend on  $\epsilon_d$  but do not rotate any more and remain at the two fixed polar angles,  $\Delta\phi = \pi/2$  ( $\epsilon_d < 0$ ) and  $\Delta\phi = 3\pi/2$  ( $\epsilon_d > 0$ ). When  $|\epsilon_d| \rightarrow \infty$ , the maximal values of  $S$  at these two polar angles decrease and go from the universal Majorana value  $S_M$  to zero. This situation is demonstrated by the black arrows representing a flow of the entropy maximum in the direction of increasing values of  $\epsilon_d$ . For large negative values of  $\epsilon_d$  one starts at the center and moves up along the  $y$ -axis when  $\epsilon_d$  increases up to  $\epsilon_d = -\epsilon_M$  where the maximal value of  $S$  is equal

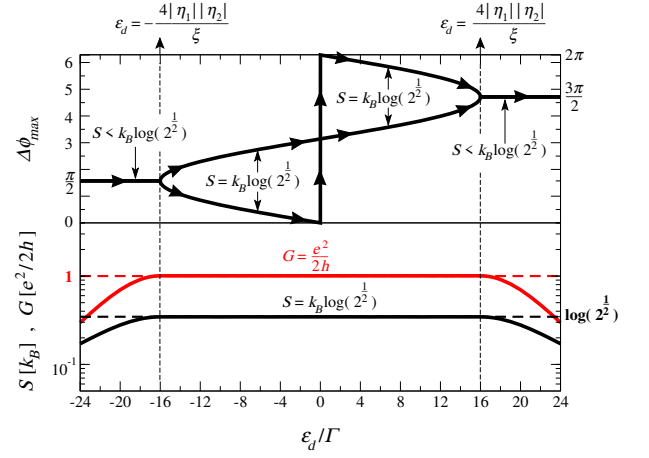


FIG. 3. Probing Majorana universality in quantum thermodynamic and transport behavior governed by nonlocal MBSs.

to the Majorana entropy  $S_M$ . After this point, when  $\epsilon_d$  increases further, the maximal value of  $S$  does not depend on  $\epsilon_d$  and remains equal to the universal Majorana entropy  $S_M$ . However, the polar angle at which it is observed splits from  $\Delta\phi = \pi/2$  into two polar angles which rotate, upon increasing  $\epsilon_d$ , on the largest polar circle  $S_M$  in the opposite directions, anticlockwise and clockwise, and merge again at the polar angle  $\Delta\phi = 3\pi/2$  when  $\epsilon_d = \epsilon_M$ . For  $\epsilon_d > \epsilon_M$  the maximal value of  $S$  again starts to depend on  $\epsilon_d$  and goes from the universal Majorana value  $S_M$  to zero when  $\epsilon_d$  goes to large positive values, that is one moves up along the  $y$ -axis from the largest polar circle  $S_M$  to the center where the flow returns to its starting point and finally stops.

In Fig. 3 we demonstrate the universality of the Majorana ground state. The parameters have the same values as in Fig. 2. Upper panel: The differences of the tunneling phases  $\Delta\phi$  corresponding to maximal values of the system's entropy  $S$  are shown as functions of  $\epsilon_d$ . As in Fig. 2, the black arrows indicate the flow of the maximal value of  $S$  in the direction of increasing values of  $\epsilon_d$ . The flow splits at the point  $\epsilon_d = -\epsilon_M$  into two flows which merge again at the point  $\epsilon_d = \epsilon_M$ . For  $\Delta\phi$  on the two flows inside the window  $|\epsilon_d| \leq \epsilon_M$  the system's entropy is equal to the Majorana value,  $S = S_M$ , and it does not depend on  $\epsilon_d$  revealing universal thermodynamic behavior induced by MBSs. Outside that universal window, that is for  $|\epsilon_d| > \epsilon_M$ , the system's entropy on the flow is no longer universal, that is it depends on  $\epsilon_d$  and its value always remains below the Majorana value,  $S < S_M$ . Lower panel: The black curve is the entropy maximum reached at  $\Delta\phi$  from the upper panel. In other words, this curve shows the system's entropy on the flow shown at the upper panel as a function of  $\epsilon_d$ . It has the Majorana plateau  $S = S_M$  for  $|\epsilon_d| \leq \epsilon_M$  and decreases when moving away from this universal window. The red curve shows the behavior of the maximal value of the linear conductance. The maximum of the linear conductance is reached also at  $\Delta\phi$  from the upper panel. Therefore,



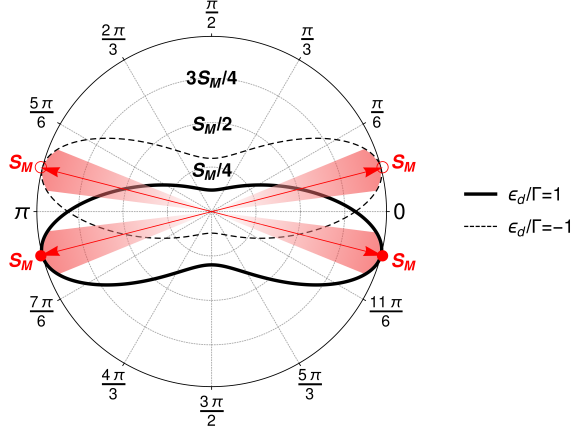


FIG. 4. A polar plot demonstrating persistence of the Majorana anisotropic character of the system's entropy at high temperatures.

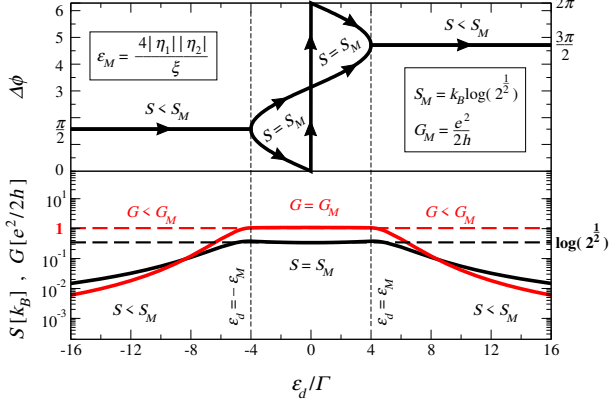


FIG. 5. Persistence of the Majorana universality of the system's entropy  $S$  and linear conductance  $G$  at high temperatures.

the linear conductance is also taken on the flow from the upper panel. The linear conductance has the Majorana plateau  $G = G_M \equiv e^2/2h$  in the same range of  $\epsilon_d$  where  $S = S_M$ . This clearly shows how the nontrivial Majorana ground state, which stores inside the nonlocality of the MBSs, uniquely determines the quantum dot linear response.

As shown in Fig. 4, a strong anisotropy of the system's entropy is observed also after an essential increase of the temperature at experimentally relevant values of the parameters. Here  $k_B T/\Gamma = 10^{-2}$ ,  $|\eta_1|/\Gamma = 1$ ,  $|\eta_2|/\Gamma = 10^{-1}$ ,  $\xi/\Gamma = 10^{-1}$ . The solid curve is for  $\epsilon_d/\Gamma = 1$  and the dashed curve is for  $\epsilon_d/\Gamma = -1$ . The red arrows correspond to  $\Delta\phi$  where  $S = S_M$ . The red angular sectors display vicinities of  $\Delta\phi$  where  $S$  is close to  $S_M$ . As can be seen, the anisotropic character and the maximal value  $S_M$  of the system's entropy are revealed even when the temperature has been raised up six orders of magnitude in comparison with Fig. 2.

Universal Majorana behavior of  $S$  and  $G$  is also ob-

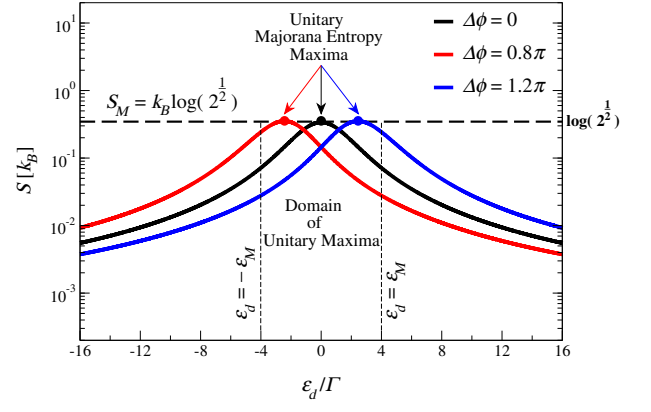


FIG. 6. Second type of experiment: revival and detection of the Majorana entropy via varying the quantum dot gate voltage  $\epsilon_d$  and at the same time keeping the tunneling phase difference  $\Delta\phi$  fixed.

served at high temperatures as demonstrated in Fig. 5. All the parameters have the same values as in Fig. 4. Upper panel: The flow of  $\Delta\phi$  on which  $S$  and  $G$  reach their maximal values. The flow is parameterized by  $\epsilon_d$ . Lower panel: The black and red curves show, respectively,  $S$  and  $G$  on the flow from the upper panel. As can be seen, the universal Majorana thermodynamic and transport behavior is robust and retains all its specific features even at very high temperatures. In particular, the universal Majorana plateaus  $S = S_M$  and  $G = G_M$  are simultaneously developed inside the window  $|\epsilon_d| \leq \epsilon_M$ . Here, for the given set of parameters, this universal window is narrowed four times in comparison with Fig. 3.

We note that, as can be seen from Figs. 2 and 4, for a given gate voltage the Majorana entropy is ruined,  $S \ll S_M$ , everywhere except for two values of the phase difference  $\Delta\phi_{max}$ , where  $S = S_M$  and two narrow angular sectors around  $\Delta\phi_{max}$  where  $S \approx S_M$ . Such behavior provides two types of experimental detection of the Majorana entropy.

First, it is clear that experiments which keep the gate voltage fixed and at the same time do not control the Majorana tunneling phases will reveal with high probability the system's entropy  $S \ll S_M$ . However, in experiments tuning the Majorana tunneling phases one will detect a maximum,  $S_{max}$ , of the system's entropy as a function of  $\Delta\phi$ . Observing  $S_{max} = S_M$  will be a fully conclusive signature of the topologically nontrivial Majorana quantum ground state which has been revived via the corresponding tunneling phases.

Second, in a setup where the Majorana tunneling phases are fixed because, due to some reasons, it is difficult to vary their values one has to keep in mind that the tunneling phase difference with an accidental finite value is in general induced during the preparation of this experimental setup. Under such circumstances we suggest to vary the quantum dot gate voltage. This is a well established experimental technique often used in more

traditional experiments. Results presented in Figs. 2 and 4 suggest that for a fixed value of  $\Delta\phi$  in experiments varying the gate voltage one will detect a maximum,  $S_{max}$ , of the system's entropy as a function of  $\epsilon_d$ . This is demonstrated in Fig. 6 where the three solid curves correspond to three different values of the tunneling phase difference:  $\Delta\phi = 0$  (black),  $\Delta\phi = 0.8\pi$  (red) and  $\Delta\phi = 1.2\pi$  (blue). The other parameters have the same values as in Fig. 4. In this type of experiment the system's entropy will reach its maximum  $S_{max}$  at some value of the gate voltage  $\epsilon_d = \epsilon_{d,max}$  located in the domain  $-\epsilon_M \leq \epsilon_{d,max} \leq \epsilon_M$  as shown in Fig. 6. Detecting  $S_{max} = S_M$  will be a totally conclusive proof of the topologically nontrivial Majorana quantum ground state which in this type of experiment has been revived via the quantum dot gate voltage. Additionally, in this type of experiment observing  $\epsilon_{d,max} \neq 0$  indicates that the tunneling phase difference is finite,  $\Delta\phi \neq 0$ . This information is important to properly analyze possible subsequent transport experiments in the same setup because they may strongly depend on  $\Delta\phi$  as it happens, for example, with the linear conductance discussed above.

#### IV. CONCLUSION

In conclusion, let us estimate the experimental relevance of the parameters used for Figs. 4-6. Obviously,  $|\epsilon_d|$  should not exceed the induced superconducting gap  $\Delta$ . For the largest energy scale  $\Gamma$  we take  $\Gamma \approx \Delta$ . Thus one should expect to observe the Majorana universality in the window  $|\epsilon_d| \leq \Gamma$ . For the parameters  $|\eta_1|$ ,  $|\eta_2|$  and  $\xi$  used to obtain the results shown in Figs. 4-6 one has  $\epsilon_M = 4\Gamma$  and thus the universal window is  $|\epsilon_d| \leq 4\Gamma$ . However, if necessary, one can properly reduce the width of the universal window changing the above parameters. For example, we have numerically checked that decreasing the parameter  $|\eta_2|$  four times,  $|\eta_2|/\Gamma = 2.5 \cdot 10^{-2}$  ( $\epsilon_M = \Gamma$ , according to Eq. (11)), leads to results similar to those shown in Figs. 4-6 but with the universal window narrowed four times,  $|\epsilon_d| \leq \Gamma$ . Concerning the temperature, for  $\Delta \approx 250 \mu\text{eV}$  (see Ref. [9]) one obtains  $T \approx 30 \text{ mK}$  as the upper limit. This means that in experiments performed at  $T \gtrsim 30 \text{ mK}$  quasiparticles above the induced superconducting gap will start to contribute to the system's macroscopic states leading to an increase of the entropy. However, for temperatures  $T \lesssim 30 \text{ mK}$  the contribution from quasiparticles above the induced superconducting gap will be significantly suppressed and thus the entropy will be essentially governed by MBSs resulting in the behavior revealed in this work. This can be seen from the expression for the entropy, Eq. (6), where the hyperbolic cosine exponentially suppresses contributions from energies  $\epsilon$  with  $|\epsilon| \gtrsim k_B T$ . Since in our work we always have  $k_B T \ll \Gamma$ , contributions from quasiparticles above the induced superconducting gap are exponentially suppressed (with a rough estimate given by  $\exp(-\Gamma/2k_B T)$ ). The latter argument is also justified by

the fact that in our noninteracting case the retarded and advanced Green's functions, Eqs. (8)-(10), do not have a temperature dependence.

In connection with practical applications of our results we note that in general Majorana tunneling phases may also be used to control qubits [37, 38] where Majorana dark states and spaces are stabilized and manipulated by means of special driven dissipative protocols. One may consider those protocols as a natural subsequent stage following the Majorana tunneling phase tuning proposed here to set up a proper initial Majorana equilibrium state of the qubit. We would like to emphasize that in this practical application the couplings between quantum dots and MBSs have been fabricated purposefully to design proper functioning of the qubit via tuning Majorana tunneling phases. As can be seen in Fig. 2 of Ref. [37], the strengths of these couplings even have the same ratio as in our Figs. 4-6, that is  $|\eta_2|/|\eta_1| = 0.1$ . Thus, although at present it may be difficult to control Majorana tunneling phases in an experiment, such a control will be necessary to manipulate Majorana qubits in future implementations of topologically protected quantum computing devices. Therefore it is also a quantum computing technology challenge for experiments to tune Majorana tunneling phases via, for example, local gates controlling the tunneling barriers between topological superconductors and quantum dots as suggested in Refs. [37, 38].

Finally, as an outlook, it would be interesting, both from theoretical and experimental points of view, to consider the case of a quantum dot with more energy levels, two or more quantum dots coupled to a topological superconductor or a topological superconductor which is not grounded (floating topological superconductor). In such setups interaction between electrons might become crucial. In particular, Coulomb blockade effects will become important and one may explore the entropy of interacting systems in the limits of a relatively large [39] or small [40, 41] value of the charging energy. For quantum dots with many energy levels one might expect that in the space of the Hamiltonian parameters there could arise a much richer structure of the domains where the system's entropy reaches the Majorana fractional values. The problem with two quantum dots coupled to a topological superconductor might be useful to study the question about the influence of a spurious tunnel coupling to any other nearby trapped state which could impact our results. In such a setup one can use gate voltages to change the relative position of the two energy levels. When the energy level in one of the two quantum dots is much lower than the energy level in the second quantum dot, one expects that the system will effectively behave as having only one quantum dot with the lowest energy level. Thus using a gate voltage to lower the energy level of the quantum dot one may significantly reduce a possible impact of nearby trapped states on our results. For a floating topological superconductor a weak Coulomb blockade leads to a smooth change of the linear conduc-

tance. From the comparison between the entropy and linear conductance in the lower panel of Fig. 5 one might also expect for weakly Coulomb blockaded topological superconductors a smooth change of the entropy. However, when Majorana tunneling phases and charging energies are both involved in formation of quantum ground states, their interplay may lead to various phenomena, like spe-

cific interaction induced values of the tunneling phases at which the Majorana entropy is reached. In any case, calculating the entropy is a promising approach which will uniquely reveal the Majorana nature of thermodynamic and transport properties of nanoscopic systems involving Majorana tunneling phases, more energy levels and floating topological superconductors.

- 
- [1] J. Alicea, “New directions in the pursuit of Majorana fermions in solid state systems,” *Rep. Prog. Phys.* **75**, 076501 (2012).
  - [2] M. Leijnse and K. Flensberg, “Introduction to topological superconductivity and Majorana fermions,” *Semicond. Sci. Technol.* **27**, 124003 (2012).
  - [3] M. Sato and S. Fujimoto, “Majorana fermions and topology in superconductors,” *J. Phys. Soc. Japan* **85**, 072001 (2016).
  - [4] R. Aguado, “Majorana quasiparticles in condensed matter,” *La Rivista del Nuovo Cimento* **40**, 523 (2017).
  - [5] R. M. Lutchyn, E. P. A. M. Bakkers, L. P. Kouwenhoven, P. Krogstrup, C. M. Marcus, and Y. Oreg, “Majorana zero modes in superconductor-semiconductor heterostructures,” *Nat. Rev. Mater.* **3**, 52 (2018).
  - [6] A. Yu. Kitaev, “Unpaired Majorana fermions in quantum wires,” *Phys.-Usp.* **44**, 131 (2001).
  - [7] R. M. Lutchyn, J. D. Sau, and S. Das Sarma, “Majorana fermions and a topological phase transition in semiconductor-superconductor heterostructures,” *Phys. Rev. Lett.* **105**, 077001 (2010).
  - [8] Y. Oreg, G. Refael, and F. von Oppen, “Helical liquids and Majorana bound states in quantum wires,” *Phys. Rev. Lett.* **105**, 177002 (2010).
  - [9] V. Mourik, K. Zuo, S. M. Frolov, S. R. Plissard, E. P. A. M. Bakkers, and L. P. Kouwenhoven, “Signatures of Majorana fermions in hybrid superconductor-semiconductor nanowire devices,” *Science* **336**, 1003 (2012).
  - [10] S. M. Albrecht, A. P. Higginbotham, M. Madsen, F. Kuemmeth, T. S. Jespersen, J. Nygård, P. Krogstrup, and C. M. Marcus, “Exponential protection of zero modes in Majorana islands,” *Nature* **531**, 206 (2016).
  - [11] H. Zhang, C.-X. Liu, S. Gazibegovic, D. Xu, J. A. Logan, G. Wang, N. van Loo, J. D. S. Bommer, M. W. A. de Moor, D. Car, R. L. M. O. het Veld, P. J. van Veldhoven, S. Koelling, M. A. Verheijen, M. Pendharkar, D. J. Pennachio, B. Shojaei, J. S. Lee, C. J. Palmstrøm, E. P. A. M. Bakkers, S. D. Sarma, and L. P. Kouwenhoven, “Quantized Majorana conductance,” *Nature* **556**, 74 (2018).
  - [12] M. Leijnse, “Thermoelectric signatures of a Majorana bound state coupled to a quantum dot,” *New J. Phys.* **16**, 015029 (2014).
  - [13] J. P. Ramos-Andrade, O. Ávalos-Ovando, P. A. Orellana, and S. E. Ulloa, “Thermoelectric transport through Majorana bound states and violation of Wiedemann-Franz law,” *Phys. Rev. B* **94**, 155436 (2016).
  - [14] L. Hong, F. Chi, Z.-G. Fu, Y.-F. Hou, Z. Wang, K.-M. Li, J. Liu, H. Yao, and P. Zhang, “Large enhancement of thermoelectric effect by Majorana bound states coupled to a quantum dot,” *J. Appl. Phys.* **127**, 124302 (2020).
  - [15] F. Chi, Z.-G. Fu, J. Liu, K.-M. Li, Z. Wang, and P. Zhang, “Thermoelectric effect in a correlated quantum dot side-coupled to Majorana bound states,” *Nanoscale Res. Lett.* **15**, 79 (2020).
  - [16] N. Bondyopadhyaya and D. Roy, “Nonequilibrium electrical, thermal and spin transport in open quantum systems of topological superconductors, semiconductors and metals,” *arXiv:2010.08336v1* (2020).
  - [17] D. E. Liu, M. Cheng, and R. M. Lutchyn, “Probing Majorana physics in quantum-dot shot-noise experiments,” *Phys. Rev. B* **91**, 081405(R) (2015).
  - [18] D. E. Liu, A. Levchenko, and R. M. Lutchyn, “Majorana zero modes choose Euler numbers as revealed by full counting statistics,” *Phys. Rev. B* **92**, 205422 (2015).
  - [19] A. Haim, E. Berg, F. von Oppen, and Y. Oreg, “Current correlations in a Majorana beam splitter,” *Phys. Rev. B* **92**, 245112 (2015).
  - [20] S. Valentini, M. Governale, R. Fazio, and F. Taddei, “Finite-frequency noise in a topological superconducting wire,” *Physica E* **75**, 15 (2016).
  - [21] S. Smirnov, “Non-equilibrium Majorana fluctuations,” *New J. Phys.* **19**, 063020 (2017).
  - [22] D. Bathellier, L. Raymond, T. Jonckheere, J. Rech, A. Zazunov, and T. Martin, “Finite frequency noise in a normal metal - topological superconductor junction,” *Phys. Rev. B* **99**, 104502 (2019).
  - [23] S. Smirnov, “Majorana finite-frequency nonequilibrium quantum noise,” *Phys. Rev. B* **99**, 165427 (2019).
  - [24] S. Smirnov, “Universal Majorana thermoelectric noise,” *Phys. Rev. B* **97**, 165434 (2018).
  - [25] S. Smirnov, “Dynamic Majorana resonances and universal symmetry of nonequilibrium thermoelectric quantum noise,” *Phys. Rev. B* **100**, 245410 (2019).
  - [26] L.-W. Tang and W.-G. Mao, “Detection of Majorana bound states by sign change of the tunnel magnetoresistance in a quantum dot coupled to ferromagnetic electrodes,” *Front. Phys.* **8**, 147 (2020).
  - [27] G. Zhang and C. Spånslätt, “Distinguishing between topological and quasi Majorana zero modes with a dissipative resonant level,” *Phys. Rev. B* **102**, 045111 (2020).
  - [28] F. Chi, T.-Y. He, J. Wang, Z.-G. Fu, L.-M. Liu, P. Liu, and P. Zhang, “Photon-assisted transport through a quantum dot side-coupled to Majorana bound states,” *Front. Phys.* **8**, 254 (2020).
  - [29] T. Simons, D. Meidan, and A. Romito, “Pumped heat and charge statistics from Majorana braiding,” *arXiv:2005.11727v1* (2020).
  - [30] S. Smirnov, “Dual Majorana universality in thermally induced nonequilibrium,” *Phys. Rev. B* **101**, 125417 (2020).
  - [31] J. Manousakis, C. Wille, A. Altland, R. Egger, K. Flensberg, and F. Hassler, “Weak measurement protocols for

- Majorana bound state identification,” *Phys. Rev. Lett.* **124**, 096801 (2020).
- [32] N. Hartman, C. Olsen, S. Lüscher, M. Samani, S. Fallahi, G. C. Gardner, M. Manfra, and J. Folk, “Direct entropy measurement in a mesoscopic quantum system,” *Nature Physics* **14**, 1083 (2018).
- [33] Y. Kleeorin, H. Thierschmann, H. Buhmann, A. Georges, L. W. Molenkamp, and Y. Meir, “How to measure the entropy of a mesoscopic system via thermoelectric transport,” *Nat. Commun.* **10**, 5801 (2019).
- [34] S. Smirnov, “Majorana tunneling entropy,” *Phys. Rev. B* **92**, 195312 (2015).
- [35] E. Sela, Y. Oreg, S. Plugge, N. Hartman, S. Lüscher, and J. Folk, “Detecting the universal fractional entropy of Majorana zero modes,” *Phys. Rev. Lett.* **123**, 147702 (2019).
- [36] A. Altland and B. Simons, *Condensed Matter Field Theory*, 2nd ed. (Cambridge University Press, Cambridge, 2010).
- [37] M. Gau, R. Egger, A. Zazunov, and Y. Gefen, “Towards dark space stabilization and manipulation in driven dissipative Majorana platforms,” *Phys. Rev. B* **102**, 134501 (2020).
- [38] M. Gau, R. Egger, A. Zazunov, and Yuval Gefen, “Driven dissipative Majorana dark spaces,” *Phys. Rev. Lett.* **125**, 147701 (2020).
- [39] L. Fu, “Electron teleportation via Majorana bound states in a mesoscopic superconductor,” *Phys. Rev. Lett.* **104**, 056402 (2010).
- [40] A. Zazunov, A. Levy Yeyati, and R. Egger, “Coulomb blockade of Majorana-fermion-induced transport,” *Phys. Rev. B* **84**, 165440 (2011).
- [41] R. Hütten, A. Zazunov, B. Braunecker, A. Levy Yeyati, and R. Egger, “Majorana single-charge transistor,” *Phys. Rev. Lett.* **109**, 166403 (2012).